

**Extended x-ray absorption fine-structure investigation  
of short-range order in  $a\text{-Ge}_{1-x}\text{Sn}_x$  alloys**

S. Pascarelli, F. Boscherini, S. Mobilio, A.R. Zanatta, F.C. Marques, I.  
Chambouleyron

## Extended x-ray-absorption fine-structure investigation of short-range order in $a\text{-Ge}_{1-x}\text{Sn}_x$ alloys

S. Pascarelli and F. Boscherini

*Istituto Nazionale di Fisica Nucleare, Laboratori Nazionali di Frascati, P.O. Box 13, I-00044 Frascati, Rome, Italy*

S. Mobilio

*Istituto Nazionale di Fisica Nucleare, Laboratori Nazionali di Frascati, P.O. Box 13, I-00044 Frascati, Rome, Italy  
and Dipartimento di Energetica, Università dell'Aquila, Roio Montelucio, L'Aquila, Italy*

A. R. Zanatta, F. C. Marques, and I. Chambouleyron

*Instituto de Física, Universidade Estadual de Campinas, P.O. Box 6165, Campinas, São Paulo 13081, Brazil*

(Received 19 March 1992)

The local environments of germanium and tin atoms in  $a\text{-Ge}_{1-x}\text{Sn}_x$  alloys ( $0.0 \leq x \leq 0.2$ ) have been investigated by measuring the extended x-ray-absorption fine structure (EXAFS) at the Ge  $K$  edge and at the Sn  $L_{III}$  edge. The measured EXAFS at both edges could be described only by assuming the presence of a mixed first coordination shell composed of both Ge and Sn atoms. Coordination numbers, bond lengths, and relative mean-square displacement values characterizing the first coordination shell around Ge and Sn atoms were obtained. It has been found that the Sn atoms are randomly distributed in the amorphous Ge network, and that metallic Sn segregation may be excluded throughout the concentration range studied. The Ge-Ge, Ge-Sn, and Sn-Sn distances were found to be independent of concentration and equal to 2.47, 2.67, and 2.80 Å, respectively. The random atomic arrangement observed is an indication that, in this concentration range and under the growth conditions adopted, the incorporation of Sn in the amorphous Ge matrix is dominated by chemical interactions, regardless of the atomic-size difference between the two atoms.

### INTRODUCTION

The study of the structure of amorphous semiconducting binary alloys is of great interest from a fundamental point of view. Specific problems to be clarified in any particular system are the following: degree of chemical ordering (examples are clustering, random distribution, and perfect chemical order), value of bond distances (in the first and possibly other coordination shells), and disorder in the bond distances. In order to have a deeper understanding of the structure, it is often useful to identify trends in these quantities as a function of relative concentration. We also note that understanding the effects of different local bonding configurations on the optical and electrical properties of these amorphous alloys is an important issue. From an applicative point of view, we see that the alloys tend to have more defects and localized gap states than elementary films, an occurrence pointing to additional disorder present in the amorphous matrix.

In order to shed light on these problems, a close examination of the local structure is of paramount importance. Extended x-ray-absorption fine-structure (EXAFS) spectroscopy is an ideal tool to study local order in amorphous semiconductors and their alloys.<sup>1-6</sup> The possibility, afforded by synchrotron radiation, of "tuning in" to a particular absorption edge and thus studying local bonding properties (bond distances, coordination numbers, and atomic mean-square relative displacements) around each particular chemical species in a binary alloy is a specific advantage of this technique.

This work is the first EXAFS study of a representative

of the family of narrow band-gap amorphous semiconductor alloys. The narrowing of the pseudogap is easily obtained by adding Sn atoms into the amorphous networks of Si or Ge. Between these two possibilities, it is reasonable to expect that  $a\text{-Ge}_{1-x}\text{Sn}_x$  films would be less defective and would have better electronic properties than the Si compounds, since the differences in atom size and in the electronic configuration are smaller between Ge and Sn than between Si and Sn. In fact, amorphous Ge-Sn films with band gaps varying between 0.4 and nearly 1 eV have been prepared and studied recently;<sup>7,8</sup> the ir optical gap is well predicted by a linear interpolation between the semiconductor band structure of Ge and the perfect semimetal band structure of  $\alpha\text{-Sn}$ .<sup>9</sup> While it is clear that hydrogenation would lead to a less defective material from the applicative point of view, the study of the present, unhydrogenated material is justified both by the expected similarity of its structure to the hydrogenated counterpart (at least in its main features) and also per se.

It is well known that, due to the size difference, the solubility of Sn in crystalline Ge is very small under equilibrium conditions.<sup>10</sup> On the other hand, in a study on the crystallization temperature of alloyed samples containing varying amounts of Sn, it has been found that amorphous Ge-Sn alloys with concentrations up to around 60 at. % of tin are stable at room temperature.<sup>11</sup> As a matter of fact, amorphous films containing up to 50 at. % tin have been prepared by the rf sputtering of pressed powder targets in argon, at a substrate temperature of  $-10^\circ\text{C}$ . Films with  $x \geq 0.6$  were partially crystal-

lized and phase separated. By means of x-ray diffraction,<sup>12</sup> it was shown that in these low- $T$  grown films, Sn entered the alloy network in a substitutional way, i.e., with a tetrahedral atomic arrangement, in a random nearest-neighbor environment.

Our samples of  $a\text{-Ge}_{1-x}\text{Sn}_x$  (with  $0.0 \leq x \leq 0.21$ ) were prepared with the same growth technique, but at a deposition temperature of 180°C. According to the crystallization studies referred to above, at this temperature a maximum Sn concentration in the network of about 40 at. % can be reached.

It is important to note at this point that the crystalline Ge-Sn system has been investigated mostly using Mössbauer spectroscopy.<sup>13-16</sup> The systems studied were of two kinds: (a) very small Sn concentrations in  $c\text{-Ge}$  (such as  $10^{18}\text{--}10^{19}\text{ cm}^{-3}$  ion-implanted  $^{119}\text{Sn}$ ) produce 100% solid solutions of Sn in Ge after adequate thermal treatments at temperatures above 300°C (however, samples that were not thermally treated always presented  $\beta\text{-Sn}$  precipitates, Sn vacancies, or other defect structures), and (b) higher Sn concentrations, up to those of the present work, always induce  $\beta\text{-Sn}$  precipitates and other defect structures that clearly appear in the Mössbauer spectra.

The structure of the present films so far has been investigated only through indirect techniques such as conversion-electron Mössbauer spectroscopy (CEMS) and Rutherford backscattering spectrometry (RBS).<sup>7,8,17</sup> At low Sn content ( $0.0 < x \leq 0.21$ ), the CEMS spectrum was fitted with just one singlet, indicating the absence of structures of defects (vacancies, dangling bonds, voids, etc.) around the Sn sites<sup>7,8</sup> and showing that all Sn atoms go substitutionally in the Ge network, i.e., in a covalent tetrahedral configuration. On the other hand, in the films at higher Sn content a second Mössbauer resonance was identified.<sup>17</sup> The analysis of its characteristics led the authors to conclude that it corresponds to a defective configuration due to the trapping of Ge vacancies by Sn atoms. The final configuration is a Sn atom in the center of a relaxed Ge divacancy bonded to six neighboring Ge atoms. In this work we directly probe the local environment of the two constituent atoms in the films at low Sn content ( $x \leq 0.2$ ), in order to give more insight into the physical mechanism which governs the accommodation of the large tin atoms in the amorphous Ge network.

## EXPERIMENT

We investigate the structure of four  $a\text{-Ge}_{1-x}\text{Sn}_x$  samples prepared by the radio-frequency sputtering of compound Ge-Sn targets in argon. The concentration range is  $0 \leq x \leq 0.21$ . The samples were grown on Al foil at a substrate temperature of 180°C. Details of the growth conditions may be found in Ref. 7. Under the growth conditions adopted, 21% Sn represents the maximum amount of Sn that could be included in the amorphous Ge matrix without the occurrence of metallic segregation, as verified by RBS measurements.<sup>7</sup> The values of concentration relative to the set of samples, obtained by measuring the relative amplitudes of the RBS signals,<sup>7</sup> are listed in the second column of Table I.

The x-ray-absorption measurements at the germanium  $K$  edge ( $E = 11\,103\text{ eV}$ ) and at the Sn  $L_{\text{III}}$  edge ( $E = 3927\text{ eV}$ ) were performed at the PULS (Progetto Utilizzazione Luce di Sincrotrone) synchrotron radiation facility of the Laboratori Nazionali di Frascati. The Adone storage ring was operated at 1.5 GeV with an average current of approximately 40 mA. The x-ray radiation was monochromatized using a Si(111) channel-cut crystal; the absorption spectra were measured by simultaneously recording the current from two ion chambers, one placed upstream and the other downstream from the sample. Samples, held in vacuum, were composed of several layers of thin film deposited on Al foil; the total  $a\text{-Ge}_{1-x}\text{Sn}_x$  thickness was chosen to optimize the signal-to-noise ratio, and was approximately  $10\text{ }\mu\text{m}$  for the Ge  $K$ -edge and  $2\text{ }\mu\text{m}$  for the Sn  $L_{\text{III}}$ -edge measurements. For the latter, two separate scans were measured for each sample and then summed to improve the signal-to-noise ratio.

## RESULTS

### Ge $K$ edge

The absorption spectra were analyzed according to standard procedures.<sup>18</sup> The pre-edge region was fitted with a linear function; the average absorption above the edge was fitted in the  $k$  range  $2.2 \leq k \leq 17.0\text{ }\text{\AA}^{-1}$  with a smooth spline formed by three cubic polynomials to simulate the atomic cross section. The EXAFS oscillations  $\chi(k)$  obtained in this way are reported in Figs. 1(a) and 1(c) for samples 2 and 4, respectively. The  $\chi(k)$ , mul-

TABLE I. Values of structural parameters obtained from the best fits of the  $k\chi(k)$  functions relative to the Ge  $K$ -edge data: coordination numbers (columns 4 and 7), interatomic distances (columns 5 and 8), mean-square relative displacements  $\sigma_{\text{sample}}^2 - \sigma_{\text{model}}^2$  (columns 6 and 9), and inelastic damping (column 10).

Sample	$x$	Model	$N_{\text{Ge-Ge}}$	$R_{\text{Ge-Ge}}$ ( $\text{\AA}$ )	$\Delta\sigma_{\text{Ge-Ge}}^2$ ( $10^{-3}\text{ }\text{\AA}^2$ )	$N_{\text{Ge-Sn}}$	$R_{\text{Ge-Sn}}$ ( $\text{\AA}$ )	$\Delta\sigma_{\text{Ge-Sn}}^2$ ( $10^{-3}\text{ }\text{\AA}^2$ )	$\gamma$ ( $\text{\AA}^{-1}$ )
1	0.00	$c\text{-Ge}$	$4.00 \pm 0.15$	$2.47 \pm 0.01$	$4.8 \pm 0.7$				
$c\text{-Ge}$		Theor	4.00 <sup>a</sup>	$2.45 \pm 0.01$	$1.2 \pm 0.6$				$1.1 \pm 0.3$
1	0.00	Theor	4.00 <sup>a</sup>	$2.47 \pm 0.01$	$5.2 \pm 0.7$				$1.1 \pm 0.3$
2	0.08	Theor	$3.60 \pm 0.20$	$2.47 \pm 0.01$	$5.2 \pm 0.7$	$0.40 \pm 0.20$	$2.69 \pm 0.03$	$8 \pm 2$	$1.1^a$
3	0.15	Theor	$3.45 \pm 0.20$	$2.47 \pm 0.01$	$4.7 \pm 0.7$	$0.55 \pm 0.20$	$2.68 \pm 0.03$	$6 \pm 2$	$1.1^a$
4	0.21	Theor	$3.20 \pm 0.20$	$2.47 \pm 0.01$	$4.2 \pm 0.7$	$0.80 \pm 0.20$	$2.67 \pm 0.03$	$5 \pm 2$	$1.1^a$

<sup>a</sup>Fixed parameter.

multiplied by  $k$ , were Fourier transformed using a Gaussian window in the  $k$  range  $3 \leq k \leq 15 \text{ \AA}^{-1}$ . The Fourier transforms all showed a single peak at approximately the same apparent position of  $R \approx 2.2 \text{ \AA}$ .

As can be seen from Figs. 1(a) and 1(c), the spectra differ strongly only at low values of  $k$  ( $k \leq 6 \text{ \AA}^{-1}$ ). This is to be expected due to the combined effect of (1) the near equality of Ge-Ge and Ge-Sn bond lengths and (2) the fact that only in this range do Sn and Ge have very different backscattering functions: Sn atoms are very strong scatterers in the  $k$  range  $3 \leq k \leq 5 \text{ \AA}^{-1}$ , as opposed to Ge atoms which scatter rather weakly in this  $k$  range. Therefore, as Sn atoms are added to the Ge matrix, the information related to the structural changes of the amorphous network will be contained mostly in the low- $k$  region of the  $\chi(k)$  function. The evolution of  $\chi(k)$  in this  $k$  region is illustrated in Fig. 2 for the whole series of samples: it shows that at least two different bond configurations are present in the EXAFS signals of the alloys. To quantify such observations, we have performed a thorough analysis in  $k$  space. This method is more direct and is generally successful when Fourier analysis is not able to resolve very close bond lengths, as in this case. The analysis shows that the first coordination shell around Ge is composed of Ge and Sn, whose relative importance varies with total Sn concentration, and values for the structural parameters relative to the two bonds, Ge-Ge and Ge-Sn, were obtained.

In order to remove noise from the experimental data, the  $k\chi(k)$  functions were filtered by performing an inverse Fourier transform in the range  $1.2 \leq R \leq 3.2 \text{ \AA}$ . The filtered  $k\chi(k)$ 's were then compared to model functions in a least-squares fitting routine, where the fitting parameters were the coordination numbers  $N$ , the bond distances  $R$ , and the mean-square relative displacements

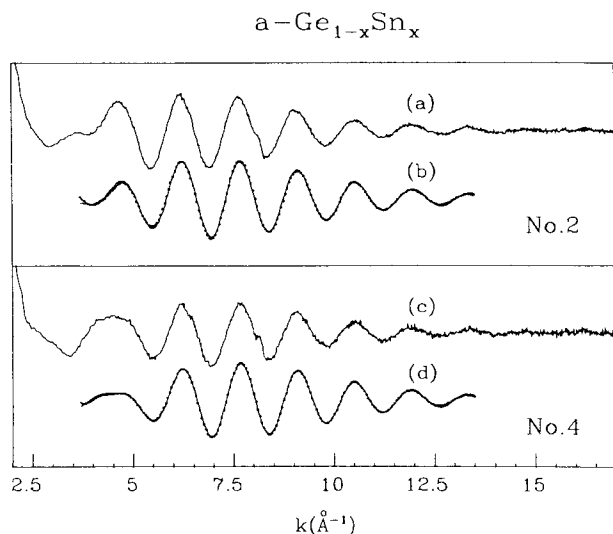


FIG. 1. Ge K-edge EXAFS and  $k$ -space data analysis for samples 2 ( $x = 0.08$ ) and 4 ( $x = 0.21$ ). (a) and (c) Raw EXAFS  $\chi(k)$ ; (b) and (d) solid line, Fourier-filtered  $\chi(k)$  multiplied by  $k$ ; dotted line, best fit to the  $k\chi(k)$  function. The scale is arbitrarily multiplied by a factor 6 for graphic purposes.

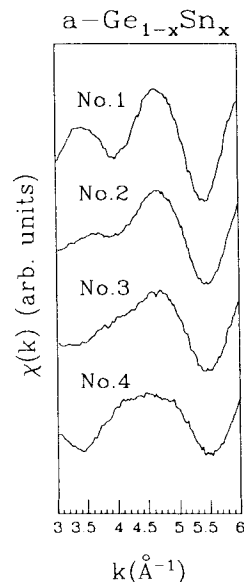


FIG. 2. Ge K-edge  $\chi(k)$ 's in the low- $k$  range for the whole set of samples, in order of increasing Sn content from top to bottom. The rise of a contribution due to a second bonding configuration is evident in passing from sample 1 to sample 4.

$\Delta\sigma^2$ . Inelastic effects were taken into account by an exponential term of the type  $e^{-2\gamma/k}$ , which in principle takes into account both the mean free path  $e^{-2R/\lambda(k)}$  and the core-hole lifetime effect  $e^{-t/\tau}$ . The latter, however, is negligible in this case, the value of the ratio  $t/\tau$  being approximately an order of magnitude lower than the expected average value of  $2R/\lambda(k)$ .

The definition of the minimized function, which is similar to a statistical  $\chi^2$  function, can be found in Ref. 19. The error bar on each parameter was obtained by changing that particular parameter until the  $\chi^2$  contribution for that parameter is doubled.

The backscattering amplitudes and phases are best obtained from EXAFS spectra of model compounds where the atomic pair desired is present in a structure which is known and, possibly, as close as possible to the unknown system in terms of chemical bonding, geometry, and distance. For instance, a natural choice as one of the model compounds is elemental crystalline Ge,  $c$ -Ge, from which data regarding the Ge-Ge scattering may be extracted. Since an equivalent crystalline counterpart for the Ge-Sn atomic pair was not available, theoretical amplitudes and phase shifts were used to simulate the Ge-Sn interaction. The outline of our fitting procedure is as follows.

Using the best-fit procedure in the  $k$  range  $3.7 \leq k \leq 13.5 \text{ \AA}^{-1}$ , the filtered spectrum of sample 1 (pure amorphous Ge,  $a$ -Ge) was compared first to a model spectrum of crystalline germanium ( $c$ -Ge) measured at  $T = 77 \text{ K}$ , and next to a model theoretical Ge-Ge signal constructed by using backscattering amplitudes and phase shifts from McKale *et al.*<sup>20</sup> and central atom phase shifts from Teo and Lee.<sup>21</sup> In the former fit, the fitting parameters were the relative coordination, the mean-square relative displacement  $\Delta\sigma^2$ , and the bond distance. The values of the best-fit parameters are reported

in Table I. The coordination number and mean-square relative displacement obtained are consistent with previous studies on sputtered<sup>5</sup> and glow discharge<sup>3</sup> *a*-Ge:H, while the bond distance is only slightly larger. The latter fit was performed in order to obtain absolute values for the mean free path  $\lambda$ . In this case  $R$ ,  $\Delta\sigma^2$ , and  $\gamma$  were left as free parameters. The values of the best-fit parameters are reported in Table I. The value of  $\gamma$  yields mean free paths ranging from 8 Å at  $k=3.7 \text{ \AA}^{-1}$  ( $E \approx 50 \text{ eV}$ ) to 30 Å at  $k=13.5 \text{ \AA}^{-1}$  ( $E \approx 700 \text{ eV}$ ). In order to confirm the mean-free-path value, the spectrum of our model compound *c*-Ge was also compared to the theoretical Ge-Ge EXAFS signal (see Table I).

As for the alloys, the model functions were built by a linear combination of two individual EXAFS signals, one due to Ge-Ge pairs and the second one to Ge-Sn pairs. Theoretical amplitudes and phase shifts (from McKale *et al.*<sup>20</sup> and Teo and Lee<sup>21</sup>) were used in the simulated EXAFS of both atomic pairs, since, as can be seen from Table I, the use of experimental or theoretical values for the Ge-Ge interaction yields similar structural parameters.

The determination of the coordination numbers presented a problem because they were found to be highly correlated to both mean-square displacements and mean free paths; reliable values for all these parameters could not be obtained without making further assumptions. The following two relationships between the fitting parameters were chosen: the total coordination number of Ge in the alloys was set to be equal to the number of nearest neighbors of *a*-Ge,  $N_{\text{Ge-Ge}} + N_{\text{Ge-Sn}} = 4$ , and the mean free paths were assumed to be equal to the value found in *a*-Ge,  $\gamma_{\text{Ge-Ge}} = \gamma_{\text{Ge-Sn}} = \gamma$ . The best-fit parameters obtained are reported in Table I. In Figs. 1(b) and 1(d) we show the fits relative to samples 2 and 4, respectively.

#### Sn $L_{\text{III}}$ edge

The analysis of these spectra was complicated by the presence of the Sn  $L_{\text{II}}$  edge at 4156 eV, which reduces the effective EXAFS energy range to about 170 eV. The pre-edge region was fitted with a linear function and the absorption above the edge with a single second-order polynomial in the  $k$  range  $3.2 \leq k (\text{\AA}^{-1}) \leq 7.4$ .

Due to the extremely restricted  $k$  range available, it was impossible to Fourier transform these spectra. The raw EXAFS were then directly compared to theoretical EXAFS signals simulating the first coordination shell. Fitting parameters now were all the structural parameters

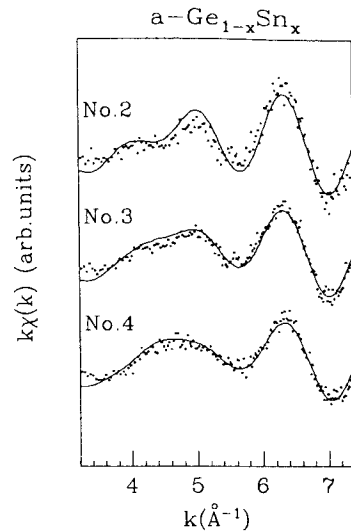


FIG. 3. Sn  $L_{\text{III}}$ -edge  $k\chi(k)$  functions for the three alloys in order of increasing Sn content from top to bottom. Dots;  $k\chi(k)$  function; solid line, best fit to the  $k\chi(k)$ .

ters characterizing the first coordination shell around Sn. We would like to point out that in all cases it was necessary to include both a Sn-Sn and a Sn-Ge contribution in order to fit the data.

The best fits were performed by fixing the total coordination equal to 4, i.e.,  $N_{\text{Sn-Sn}} + N_{\text{Sn-Ge}} = 4$ . Moreover, a  $k$ -independent inelastic damping term  $e^{-2R/\lambda}$  (with  $\lambda$  equal for the two atomic pairs,  $\lambda_{\text{Sn-Sn}} = \lambda_{\text{Ge-Sn}} = \lambda$ ) was assumed: This is not too restrictive due to the limited  $k$  range. In Fig. 3 we show the results of the fits on the three alloys, and the best-fit parameters obtained are listed in Table II. While the values of bond distances are quite reproducible, the coordination numbers have a higher error bar; this is to be related to the restricted  $k$  range.

#### DISCUSSION

The most obvious feature of the values reported in the two tables is the constancy of interatomic distances to within  $\pm 0.015 \text{ \AA}$ ; of all the quantities reported, interatomic distances have the smallest error and greatest reliability. The values of all bond lengths as a function of composition are reported in Fig. 4. The constancy of bond lengths has also been observed in other amorphous semiconductor alloys. EXAFS measurements on *a*- $\text{Si}_{1-x}\text{Ge}_x$ :H<sup>3</sup>, *a*- $\text{Si}_{1-x}\text{N}_x$ :H<sup>4</sup>, *a*- $\text{Ge}_{1-x}\text{N}_x$ :H<sup>5</sup>, and *a*-

TABLE II. Values of structural parameters obtained from the best fits of the  $k\chi(k)$  functions relative to the Sn  $L_{\text{III}}$ -edge data: coordination numbers (columns 3 and 6), interatomic distances (columns 4 and 7), mean-square relative displacements  $\sigma_{\text{sample}}^2 - \sigma_{\text{model}}^2$  (columns 5 and 8), and mean free path (column 9).

Sample	Model	$N_{\text{Sn-Sn}}$	$R_{\text{Sn-Sn}}$ (Å)	$\Delta\sigma_{\text{Sn-Sn}}^2$ ( $10^{-3} \text{ \AA}^2$ )	$N_{\text{Sn-Ge}}$	$R_{\text{Sn-Ge}}$ (Å)	$\Delta\sigma_{\text{Sn-Ge}}^2$ ( $10^{-3} \text{ \AA}^2$ )	$\lambda$ (Å)
2	Theor	0.0–0.3	2.81±0.04	3±3	3.7–4.0	2.66±0.03	7±3	10–15
3	Theor	0.55±0.40	2.80±0.04	3±3	3.45±0.40	2.67±0.02	6±3	11±3
4	Theor	0.80±0.25	2.78±0.04	3±3	3.20±0.25	2.65±0.02	5±3	9±3

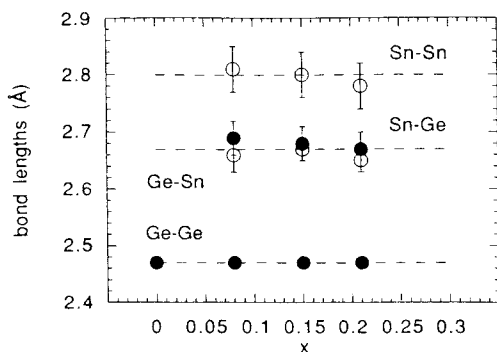


FIG. 4. Average bond lengths as a function of composition  $x$  in the  $a\text{-Ge}_{1-x}\text{Sn}_x$  alloys as deduced from Ge  $K$ -edge EXAFS (solid dots) and from Sn  $L_{\text{III}}$ -edge EXAFS (open dots). Note that the Ge-Sn distance obtained from the two sets of measurements (at the Ge  $K$  edge and at the Sn  $L_{\text{III}}$  edge) is equivalent, a further proof of the reliability of the EXAFS technique in the determination of bond-length values.

$\text{Si}_{1-x}\text{C}_x\text{:H}^6$  have shown that a common feature of all these alloys is the constancy of the average bond length as a function of composition. The relaxation of the interatomic distances to their "molecular" values can be seen as a consequence of the absence of long-range-order constraints on bond lengths in the amorphous network.

In the  $a\text{-Ge}_{1-x}\text{Sn}_x$  films the Ge-Ge bond length is equal to  $(2.47 \pm 0.01)$  Å, being slightly larger than the crystalline value of 2.45 Å, while the Ge-Sn bond length is equal to  $(2.67 \pm 0.03)$  Å, which compares well with the sum of the two covalent radii of 2.64 Å. The simplest conclusion that can be drawn from this value is that when Sn is included in the  $a\text{-Ge}$  network, its bonding to Ge is determined mostly by Ge-Sn local interactions. The Ge-Sn interatomic distance has been double checked, since the values obtained from both sets of data, at the Ge  $K$  edge and at the Sn  $L_{\text{III}}$  edge, are equivalent. This is a further proof of the reliability of the values of bond lengths obtained with this technique. As for the Sn-Sn bond, the value of  $(2.80 \pm 0.04)$  Å is equal to the crystalline value in  $\alpha\text{-Sn}$ , the phase of tin stable at low temperature ( $T < 13^\circ\text{C}$ ), in which tin atoms are covalently bonded in a diamond structure. This fact shows the absence of metallic  $\beta\text{-Sn}$  clusters ( $R_{\text{Sn-Sn}} = 3.02$  Å), but also indicates that the interaction between Sn atoms is influenced by the amorphous Ge tetrahedral environment in which they are incorporated.

The local environments of both Ge and Sn in the films can be examined from the values reported in Tables I and II. The presence of octahedrally coordinated Sn sites, already observed through CEMS at higher Sn contents,<sup>17</sup> unfortunately cannot be investigated due to the much lower sensitivity of the technique. The number of these defects, however, is very small, considering that the singlet is barely detectable with the CEMS sensitivity limits (about  $5 \times 10^{18} \text{ cm}^{-3}$ ). In our case, at the Sn  $L_{\text{III}}$  edge, an estimate of the sensitivity is given by the errors on the values of the coordination numbers.

In order to study the arrangement of Ge and Sn on the sites of the amorphous network, we compared experimen-

tal normalized coordination numbers with theoretical values calculated in the two extreme cases of a completely random distribution of bonds and of a totally chemically ordered network (TCON).<sup>22</sup> In the former case the distribution of bonds is purely statistical and the coordination numbers are proportional to composition, while in the latter, the distribution is found by maximizing the number of heteroatomic bonds at all compositions. In particular, a TCON is characterized by the absence of homopolar bonds between minority-type atoms, i.e., Sn-Sn bonds are forbidden in  $a\text{-Ge}_{1-x}\text{Sn}_x$  alloys for  $x < 0.5$ . This comparison enabled us to test for the presence of chemical order in the films. The results obtained from the data at the Ge  $K$  edge and at the Sn  $L_{\text{III}}$  edge are reported in Figs. 5(a) and 5(b), respectively. The values of Fig. 5 lead us to conclude that when Sn atoms are introduced in the  $a\text{-Ge}$  network, the resulting distribution of bonds is random, and chemical ordering in the films can be excluded.

This result is important because it excludes the presence of metallic clustering in the alloys. The fact that the Sn-Sn bonds appear to be randomly distributed in the  $a\text{-Ge}$  network excludes segregation of Sn atoms in  $\beta\text{-Sn}$  metallic clusters at these compositions, as observed by RBS.<sup>7</sup> To this end, we must recall that previous RBS studies on our samples have in fact shown that metallic segregation may occur for Sn concentrations as low as 20 at. %, but only in samples grown with the presence of hydrogen in

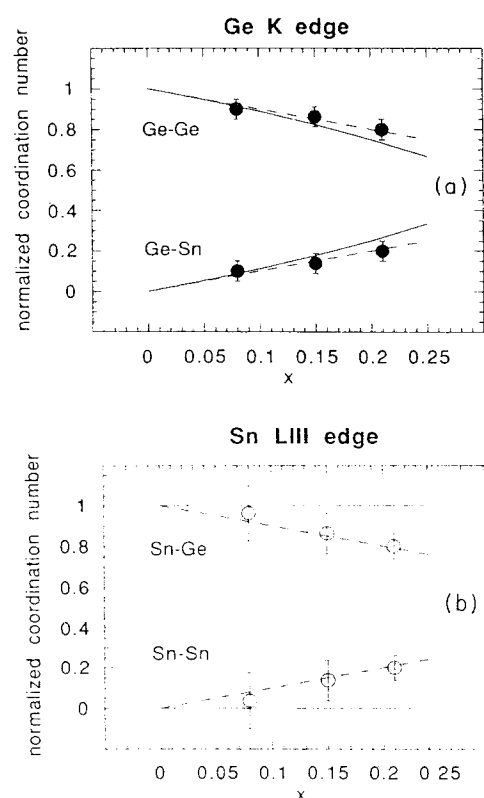


FIG. 5. Normalized coordination number  $N_{A,B}/4$  as a function of composition  $x$ . The dashed and solid lines refer to a random distribution of bonds and to a totally chemically ordered network, respectively. (a) At the Ge  $K$  edge ( $A = \text{Ge}$ ,  $B = \text{Ge}$ , Sn); (b) at the Sn  $L_{\text{III}}$  edge ( $A = \text{Sn}$ ,  $B = \text{Ge}$ , Sn).

the reaction chamber.<sup>8</sup>

We now compare the present results with previous structural studies of amorphous binary alloys. The problem of chemical ordering has been studied in a variety of Si- and Ge-based binary amorphous alloys. Based on the results of EXAFS measurements, a random distribution of atoms was found in  $a\text{-Si}_{1-x}\text{Ge}_x\text{:H}^3$ , while in  $a\text{-Si}_{1-x}\text{N}_x\text{:H}^4$ ,  $a\text{-Ge}_{1-x}\text{N}_x\text{:H}^5$ , and  $a\text{-Si}_{1-x}\text{C}_x\text{:H}^6$ , strong tendencies toward chemical order were observed. An explanation for this major difference is immediately evident by comparing the relative importance of the "chemical" term (related to the electronegativity difference of the two constituent atoms) in the calculation of the enthalpy of mixing in these binary systems. The Pauling electronegativities for these atoms in fact go from 1.8 for Si, Ge, and Sn, to 2.5 for C and 3.0 for N. The ionicity of the Si-Ge bond is therefore very small compared to the Si-N, Ge-N, and the Si-C bonds. We note here that studies of the stability of ordered Si-C and Si-Ge model alloys using first-principles, self-consistent, total-energy calculations<sup>23</sup> show that the Si-C bond is stabler than the average of the Si-Si and C-C bonds, while the opposite is true for the Si-Ge bond. The reason for this fundamental difference is apparent from the calculated charge densities: whereas in SiC the direction of charge transfer mandated by the atomic electronegativities (Si→C) coincides with increased cohesion (diamond having a larger cohesive energy than Si), in SiGe there is little change in the charge density around the atoms (i.e., no charge transfer). The same argument can be extended to the Si-N and Ge-N systems, which are "chemically" very similar to the Si-C system, also taking into account the higher cohesive energy of the N-N bond with respect to both the Si-Si and the Ge-Ge bond. Based on these considerations, the Ge-Sn system is expected to behave like the Si-Ge system, consistent with observation.

While it is true that electronegativity has a great

influence in chemical ordering, another key aspect is atom size. Clearly, from this point of view, the Ge-Sn system is not directly comparable to the Si-Ge system. The atom size is almost identical in the second case and both elements are miscible in any proportion, even in the crystalline structure. On the contrary, any attempt to put Sn in Ge is accompanied by segregation. The only way to introduce substitutional Sn in Ge is by the fast condensation of the vapor phase, which is the method we used, but the amount of Sn which can be accommodated decreases with increasing substrate temperature, as expected. Increasing substrate temperature increases adatom mobility, leading to an arrangement of bonds which is expected to depart from a random distribution at high growth temperatures.

## CONCLUSIONS

The main conclusion of this study is that at a substrate temperature of 180°C, departures from a random distribution of bonds are still not observed, and therefore the relative atomic arrangement in the  $a\text{-Ge}_{1-x}\text{Sn}_x$  alloys is determined mainly by the similar electronegativities of Ge and Sn, atom-size effects being negligible. Sn atoms enter the  $a\text{-Ge}$  network in a substitutional way at these concentrations, and all interatomic distances are found to be independent of concentration. The Ge-Sn bond length, close to the sum of the two covalent radii, indicates that the inclusion of Sn atoms in the  $a\text{-Ge}$  network is mostly determined by Ge-Sn local interactions, while the value found for the Sn-Sn bond indicates that the interaction between the Sn atoms is strongly influenced by the amorphous Ge tetrahedral environment in which they are incorporated.

## ACKNOWLEDGMENTS

This work has been partially supported by FAPESP and CNPq, Brazil.

<sup>1</sup>D. Sayers, E. Stern, and F. W. Lytle, *Phys. Rev. Lett.* **27**, 1204 (1971).

<sup>2</sup>P. A. Lee, P. H. Citrin, P. Eisenberger, and B. M. Kincaid, *Rev. Mod. Phys.* **53**, 769 (1981).

<sup>3</sup>L. Incoccia, S. Mobilio, M. G. Proietti, P. Fiorini, C. Giovannella, and F. Evangelisti, *Phys. Rev. B* **31**, 1028 (1985).

<sup>4</sup>S. Mobilio and A. Filipponi, *J. Non-Cryst. Solids* **97&98**, 365 (1987).

<sup>5</sup>F. Boscherini, A. Filipponi, S. Pascarelli, F. Evangelisti, S. Mobilio, F. C. Marques, and I. Chambouleyron, *Phys. Rev. B* **39**, 8364 (1989).

<sup>6</sup>S. Pascarelli, F. Boscherini, S. Mobilio, and F. Evangelisti, *Phys. Rev. B* **45**, 1650 (1992).

<sup>7</sup>I. Chambouleyron, F. C. Marques, J. P. de Souza, and I. J. R. Baumvol, *J. Appl. Phys.* **63**, 5596 (1988).

<sup>8</sup>I. Chambouleyron and F. C. Marques, *J. Appl. Phys.* **65**, 1597 (1989).

<sup>9</sup>M. L. Cohen and T. K. Bergtresser, *Phys. Rev.* **141**, 789 (1966).

<sup>10</sup>F. A. Trumbore, *J. Electrochem. Soc.* **103**, 597 (1956).

<sup>11</sup>R. J. Temkin and W. Paul, in *Amorphous and Liquid Semiconductors*, edited by J. Stuke and W. Brenig (Taylor & Francis, London, 1974), p. 1193.

<sup>12</sup>R. J. Temkin, G. A. N. Connell, and W. Paul, *Solid State*

*Commun.* **11**, 1591 (1972).

<sup>13</sup>G. Weyer, S. Damgaard, J. W. Petersen, and J. Heinemeier, *Phys. Lett. A* **76**, 321 (1980).

<sup>14</sup>L. K. Nanver, G. Weyer, and B. I. Deutsch, *Z. Phys. B* **47**, 103 (1982).

<sup>15</sup>N. I. Lisichenko, N. N. Petrichenko, and A. A. Yakunin, *Fiz. Tverdogo Tela (Leningrad)* **17**, 2330 (1975) [*Sov. Phys.—Solid State* **18**, 183 (1976)].

<sup>16</sup>P. P. Seregin, S. R. Bakhchieva, M. G. Kekua, and A. V. Petrov, *Fiz. Tverdogo Tela (Leningrad)* **21**, 1236 (1979) [*Sov. Phys.—Solid State* **21**, 718 (1979)].

<sup>17</sup>I. Chambouleyron, F. C. Marques, P. H. Dionisio, I. J. R. Baumvol, and R. A. Barrio, *J. Appl. Phys.* **66**, 2083 (1989).

<sup>18</sup>B. Lengeler and P. Eisenberger, *Phys. Rev. B* **21**, 4507 (1980).

<sup>19</sup>F. W. Lytle, D. E. Sayers, and E. A. Stern, *Physica B* **158**, 701 (1989).

<sup>20</sup>A. G. McKale, B. W. Veal, A. P. Paulikas, S. K. Chan, and G. S. Knapp, *J. Am. Chem. Soc.* **110**, 3763 (1988).

<sup>21</sup>B. K. Teo and P. A. Lee, *J. Am. Chem. Soc.* **101**, 2815 (1979).

<sup>22</sup>G. S. Cargill III and F. Spaepen, *J. Non-Cryst. Solids* **43**, 91 (1981).

<sup>23</sup>J. L. Martins and A. Zunger, *Phys. Rev. Lett.* **56**, 1400 (1986).